ISSN 2079-1704. Хімія, фізика та технологія поверхні. 2016. Т. 7. № 1. С. 86-96

UDC:539.143.43:620.3 doi: 10.15407/hftp07.01.086

V.M. Gun'ko [1], V.V. Turov [1], T.V. Krupska [1], A.P. Golovan [1], E.M. Pakhlov [1], M.D. Tsapko [2], J. Skubiszewska-Zięba [3], B. Charmas [3]

STATES OF WATER *VS.* TEMPERATURE IN DIFFERENTLY HYDRATED KEFIR GRAINS

[1] Chuiko Institute of Surface Chemistry of National Academy of Sciences of Ukraine
17 General Naumov Str., Kyiv, 03164, Ukraine, E-mail: vlad_gunko@ukr.net
[2] Kyiv Taras Shevchenko National University, Faculty of Chemistry
60 Volodymyrska Str., Kyiv, 01030, Ukraine, E-mail: nmrlab2007@ukr.net
[3] Maria Curie-Skłodowska University, Faculty of Chemistry
3 Maria Curie-Skłodowska pl., Lublin, 20031, Poland, E-mail: jskubisz@o2.pl

Kefir grains (KG) were studied using low-temperature ^{1}H NMR spectroscopy, DSC, and thermogravimetry to analyse the influence of the hydration degree on the properties of water bound in KG, as well as effects of dispersion media (air, weakly polar $CDCl_3$, $CDCl_3$ + F_3CCOOD) and temperature. An increase in water content added to dried KG results in changes in water structure and supramolecular organisation in bacteria, low- and high-molecular components of KG. Five types of water are observed in KG: (i) weakly associated water characterised by a low value of the chemical shift of proton resonance δ_H = 1–2 ppm; (ii) strongly associated water at δ_H = 4–5.5 ppm (similar to that of bulk water), (iii) weakly bound water frozen at 265 K < T < 273 K; (iv) strongly bound water frozen at 200 K < T < 265 K; and (v) bulk water, which does not directly interact with bacteria, cells, and macromolecules. NMR cryoporometry and thermoporometry based on both DSC and thermogravimetry give close results and show detailed changes in intracellular and extracellular organisations of water and other low-molecular weight compounds due to hydration/dehydration, addition of weakly polar ($CDCl_3$) or strongly polar (F_3CCOOD) compounds, heating or freezing.

Keywords: *kefir grains, weakly associated and strongly associated water*

INTRODUCTION

Gelatinous, irregularly-shaped kefir grains (KG) are formed by a symbiotic combination of yeasts, acetic acid bacteria and lactic acid bacteria (LAB) [1–5]. KG have gel-like shells consisting of polysaccharides and some other compounds. Kefir is characterised by certain antimicrobial [4], antioxidant [6], and disease-resistant activities [1, 2] depending on KG composition, amounts and organisation of water. Water state and temperature behaviour play an important role in KG [1, 6, 7]. Water located in cells and bacteria and between them (*i.e.* bulk water) can be in a strongly structured (bound) state [8–10]. The confined space effects can result in significant changes in the properties of liquids as solvents, since the activity and molecular mobility decreases in comparison with the bulk liquids. These changes depend on water content, topology and chemistry of surroundings, presence and content of solutes (salts, small molecules as saccharides, fats, amino acids, *etc*.) and temperature [9, 11]. Bacteria used in food industry can be stored in freeze-dry state [10]. Therefore, the behaviour of water bound in bioobjects stored at T < 273 K is of interest.

There are several methods such as nuclear magnetic resonance (NMR) spectroscopy, differential scanning calorimetry (DSC), X-ray diffraction, thermogravimetry, dielectric relaxation spectroscopy, and thermally stimulated depolarisation current, which can give useful information on the structure, temperature and interfacial behaviours, and other properties of water in bioobjects [9, 11–13]. This is of importance since practically all properties of water are unusual in comparison of them for hydrides of other elements, *e.g.* SH_2, NH_3, CH_4, *etc* [10]. In the case of a large part of bulk water in bio-objects, it is difficult to study the properties of bound water. Therefore, the systems with small and controlled content of water are more appropriate to analyse the temperature behaviour of water bound in cells and bacteria.

The aim of this work was to study the properties of water bound in kefir grains depending on water content, dispersion media with air or weakly organic solvent $CDCl_3$ and the presence of trifluoroacetic acid F_3CCOOD (TFAA) using low-temperature ^{1}H NMR, DSC, and TG methods.

EXPERIMENTAL

Kefir grains (KG) prepared by fermentation of whole milk were washed out by distilled water, placed onto filter paper and dried at room temperature for 1 h. For NMR measurements, the samples were dried at 330 K in air. The residual amount of water was $h = 0.3$ g per gram of dry KG. Partial re-hydration of KG was carried out by addition of certain amounts of water ($h = 0.8$ g/g). Before DSC measurements, air-dry KG were heated at 380 K for 20 min, and then certain amounts of water were added to KG ($h = 0.3$, 0.5, 0.7 and 1 g/g).

Microscopic images were recorded using DualBeam Quanta 3D FEG (FEI, USA) in the condition of low vacuum (accelerating voltage 10 kV, magnification from ×65 to ×65000) applied to samples with deposition of a thin film of palladium and gold. Qualitative and quantitative elemental analysis was made using an EDS detector coupled with a microscope (EDAX, USA). Composition (according to the EDS data) of dry kefir grains (in at. %) is C (66.79), O (22.96), N (7.37), P (1.36), S (0.44), Ca (0.35), K (0.19), Al (0.18), Cl (0.16), Mg (0.15), and Si (0.04).

^{1}H NMR spectra of static samples (placed into 5 mm NMR ampoules) with various amounts of water in various dispersion media (air, $CDCl_3$, $CDCl_3 + F_3CCOOD$) were recorded using a Varian 400 Mercury spectrometer (magnetic field 9.4 T, bandwidth 20 kHz) utilising eight 60^o pulses of 1 μs duration. Relative mean errors were less than ±10 % for ^{1}H NMR signal intensity for overlapped signals, and ±5 % for single signals. Temperature control was accurate and precise to within ±1 K. The accuracy of integral intensities was improved by compensating for phase distortion and zero-line nonlinearity with the same intensity scale at different temperatures. To prevent supercooling of samples, the beginning of spectra recording was at $T = 210$ K. Samples precooled to this temperature for 10 min were then heated to 280 K at the rate of 5 K/min with steps $\Delta T = 10$ K or 5 K at the heating rate of 5 K/min for 2 min. They were maintained at a fixed temperature for 9 min before data acquisition at each temperature for 1 min [9, 13].

The applications of low-temperature ^{1}H NMR spectroscopy and NMR cryoporometry, based on the freezing point depression of liquids located in pores depending on the pore size [11], to numerous objects were described in detail elsewhere [9, 13]. Note that high-molecular weight compounds do not contribute the ^{1}H NMR spectra recorded here for static samples due to a large difference in the transverse relaxation time of liquid (mobile) small compounds (water, sugars, *etc.*) and macromolecules or solids and due to a narrow bandwidth (20 kHz) of the spectrometer [9]. In our calculations, the constant k_{GT} in the Gibbs-Thomson equation describing the freezing/melting point depression due to confined space effects was equal to 60 K nm.

Differential scanning calorimetry (DSC) measurements of interactions of kefir grains with water and *n*-decane were carried out using a PYRIS Diamond (Perkin Elmer Instruments, USA) differential scanning calorimeter at the constant heating/cooling rate of 10 K/min. PYRIS Diamond DSC was calibrated at different heating rates using such standard samples as distilled water (melting temperature $T_m = 273$ K) and standard indium sample ($T_m = 429.6$ K) supplied by the producer and using the standard calibration procedure recommended by the supplier.

Similar to the NMR cryoporometry, the DSC melting thermograms can be used in the DSC thermoporometry for structural characterisation of the materials. Bound liquids demonstrate the freezing-melting point depression in the DSC thermograms that can be treated as described elsewhere [14].

Thermogravimetry (TG) measurements of air-dry kefir grains were carried out at 293 to 1273 K in air or nitrogen atmosphere using a Derivatograph-C (Paulik, Paulik & Erdey, MOM, Budapest) apparatus at the heating rate of 10 K/min. The thermoporometry method was applied to the TG data for air-dry kefir grains as described elsewhere [9, 15].

The IR spectra of differently preheated KG samples (thin plates ~20 mg) over the 4000–300 cm^{-1} range (at 4 cm^{-1} resolution) were recorded in transmittance mode using a Specord M80 (Carl Zeiss, Jena) spectrometer.

RESULTS AND DISCUSSION

Observed supracellular and cellular structures observed in kefir grains (Fig. 1) show their nonuniform morphology of a great complexity. Deviation of the cellular shapes (Fig. 1 d) can be caused by drying of cells. This suggests that intracellular and extracellular structures of water can demonstrate complex temperature behaviour, which is typical for cellular objects and can strongly depend on the water content.

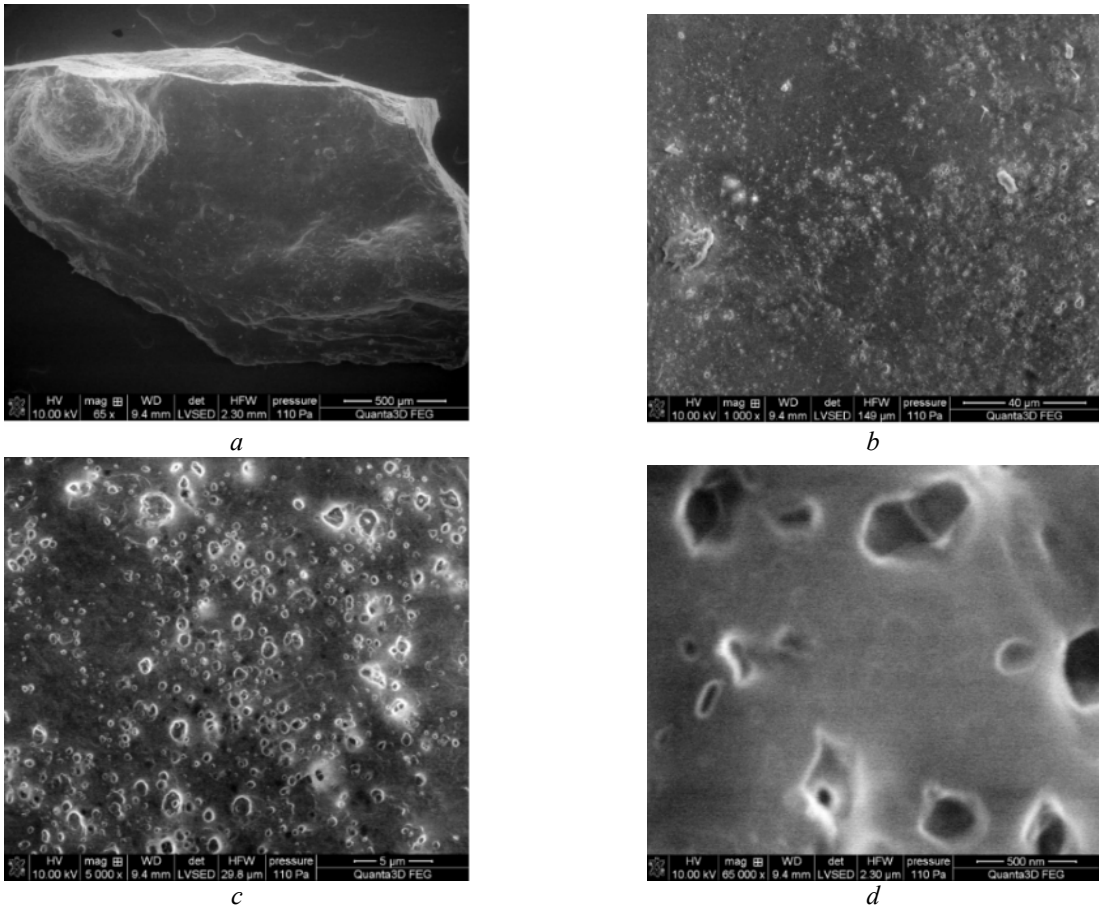

Fig. 1. SEM images of dried kefir grains at various magnifications (from ×65 to ×65000) at scale bar of: (*a*) 500 μm, (*b*) 40 μm, (*c*) 5 μm, and (*d*) 0.5 μm

The TG thermograms of initial, dried, and hydrated KG recorded upon heating from 293 to 1273 K (Fig. 2) show several characteristic parts. The first one from 293 to 398 K corresponds to desorption of bulk or weakly bound water (WBW) and other low-molecular weight compounds (*e.g.* CO_2, alcohol, *etc*.). The second range (393–473 K) is due to desorption of structured strongly bound water (SBW) and decomposition of a portion of macromolecules. The third range (473–673 K) with rapid loss of the weight corresponds to dehydration and decomposition of biomacromolecules (*e.g.* polysaccharides, *etc*.). At $T > 673$ K, there is significant difference in the TG/DTG curves recorded in the air and nitrogen atmosphere. For the former, oxidation processes are characteristic in contrast to the latter (curves *3* and *7*). Therefore, the weight loss in air is much greater ~93.4 wt. % for dry KG (*i.e.* ~6 wt. % corresponds to mineral components in dried kefir grains, see element composition of them) at 1273 K than that in the nitrogen atmosphere without access of oxygen ~70 wt. %, in which the processes are stopped on the carbonisation stage (*i.e*. formation of char).

The IR spectra (Fig. 3) show that heating of KG results in the loss of water, since intensity of a broad band at 3700–2500 cm^{-1} decreases with increasing preheating temperature. However, even after preheating at 413 K for 2 h the KG keep the main structural features, despite thermal inactivation of bacteria and cells. A broad complex band at 1200–1000 cm^{-1} related to C–O–C and C–O is characteristic for carbohydrates. Bands at 1700–1500 cm^{-1} are linked to the C=O and C=C stretching vibrations and the δ_{CN} bending vibrations and C–H overtones. The bands at 1460 and 1400 cm^{-1} can be assigned to the CH_2 deformation and to vibrations of the amino acid side chains, respectively. A decrease in intensity of all bands observed can be due to desorption of low-molecular weight organics (e.g., saccharides) in parallel to desorption of water.

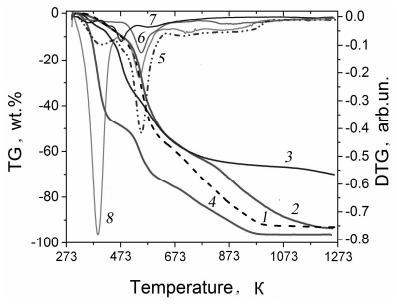

Fig. 2. Thermograms (TG (*1–4*) and differential TG (*5–8*) curves) of (*1, 5*) initial, (*4, 8*) wetted (water:dry KG = 1:1), dried kefir grains upon heating in (*2, 6*) air and (*3, 7*) nitrogen atmosphere

Detailed information on the temperature behaviour of water bound in KG at various hydration degrees in air, chloroform or chloroform + TFAA dispersion media was obtained using low-temperature ^{1}H NMR spectra of static samples (to avoid signals of immobile phases) (Figs. 4 and 5) and DSC (Figs. 6 and 7).

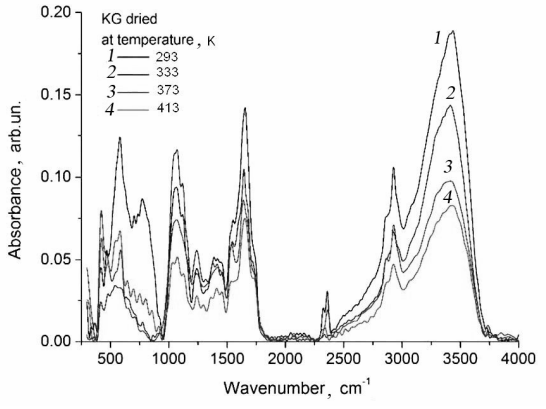

Fig. 3. IR spectra of KG dried at room temperature for 4 days (curve *1*) and at 333 (*2*), 373 (*3*), and 413 (*4*) K for 2 h

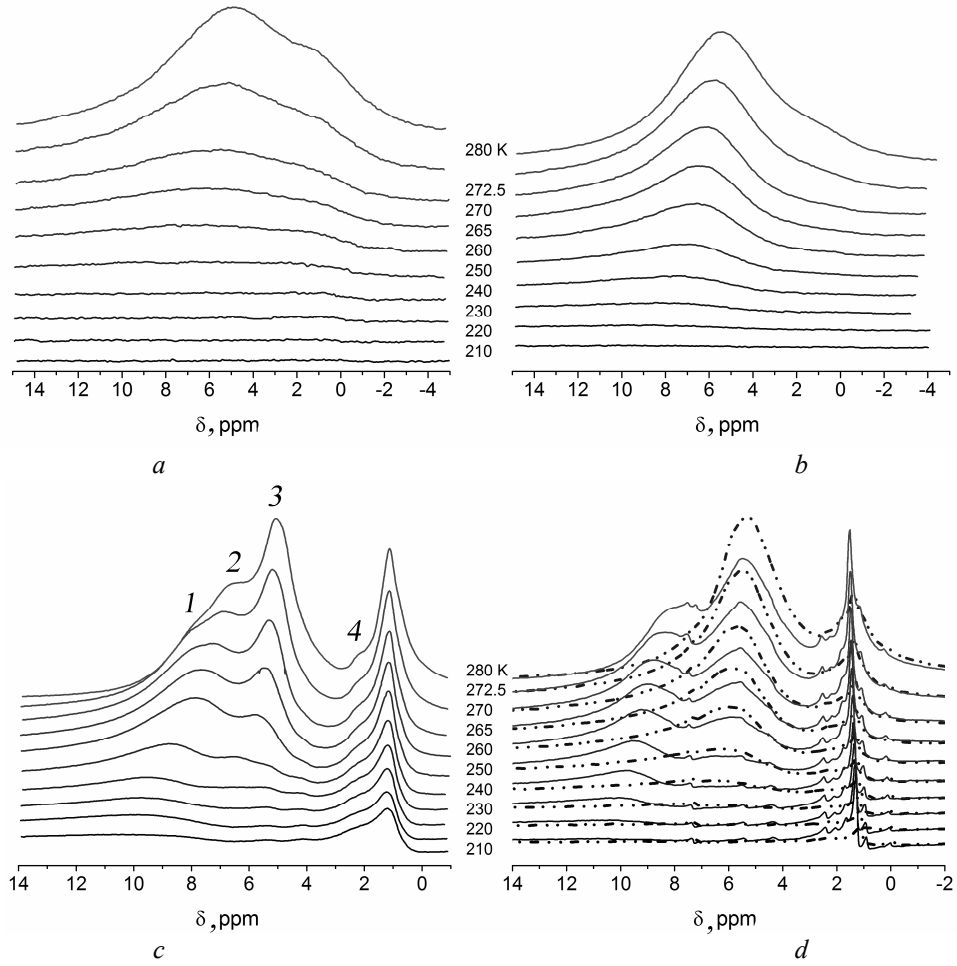

Fig. 4. ^{1}H NMR spectra of water bound in KG recorded at different temperatures and different hydration degree h = (*a*, *c*) 0.3 g/g, (*b, d*) 0.8 g/g in various dispersion media: (*a, b*) air, (*d*) $CDCl_3$ (dotted-dashed lines), and (*c, d* solid lines) $8CDCl_3$ + 1TFAA

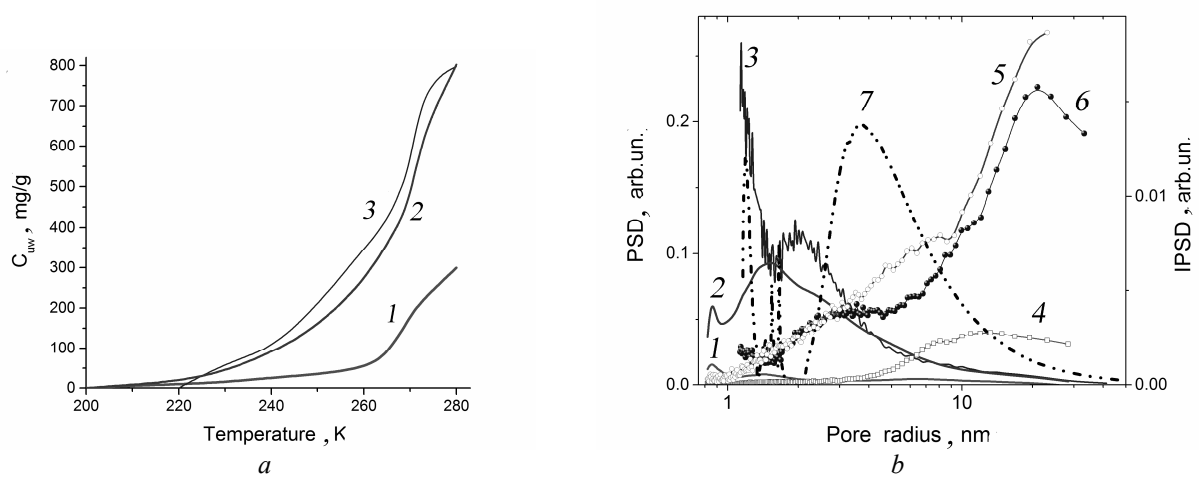

Fig. 5. (*a*) Temperature dependence of content of unfrozen water (C_{uw}) for samples in air (curve 1 – h = 0.3 g/g, and curve 2 – h =0.8 g/g) and in chloroform-d at h =0.8 g/g (curve 3); and (*b*) corresponding differential (curves 1–3) and incremental (curves 4–6) distribution functions of sizes of water structures filling "pores" in KG. Curve 7 corresponds to TG thermoporometry calculation for sample at h = 1 g/g

For KG in air, two ^{1}H NMR signals are observed at the chemical shift of proton resonance $\delta_H = 5$ and 1.5 ppm (Fig. 4 *a, b*). Signal at $\delta_H = 5$ ppm can be assigned to strongly associated water (SAW), in which the average number of the hydrogen bonds per molecule is close to that in bulk water [9]. The second signal at 1.5 ppm can be attributed to methylene and methyl groups in low-molecular weight compounds (saccharides, phospholipids, fat acids, *etc*.), as well as to weakly associated water (WAW). WAW corresponds to water structures at the average number of the hydrogen bonds per water molecule $n_H \leq 1$ for the hydrogen atoms. Intensity of both signals decreases with decreasing temperature due to freezing out of fractions of water molecules (Fig. 5 *a*) differently interacting with surroundings and being under different confined space effects. The latter allows us to calculate the distribution functions of sizes of water structures bound in KG (Fig. 5 *b*). Note that relative intensity of signal at 5 ppm increases with decreasing temperature (Fig. 4 *b*). This can suggest that the contribution of WAW into signal at 1.5 ppm is not predominant since typically WAW is frozen out more slowly than SAW due to stronger confined space effects for the former [9].

In chloroform dispersion medium (Fig. 4 *c, d*), signal at 1.5 ppm splits and shows fine structure at 0.8–3.0 ppm. This suggests the presence of several sources of this signal, *i.e.* WAW and low-molecular weight organics. To separate water and organics with CH_2 and CH_3 groups, relatively strong acid TFAA was added (Fig. 4 *c, d*). Mixtures with acids and water (with fast proton exchange since initial TFAA was in a deuterated form) are characterised by a significant downfield shift [16].

For a sample at a lower value of h (Fig. 4 *c*), three signals of SAW are observed. For pure TFAA, δ_H is equal to 11.5 ppm. Therefore, observed SAW structures can be attributed to different solutions of TFAA from maximal content at signal 1 to minimal one at signal 3, since the value of δ_H for signal 3 is close to that of pure water. Consequently, a significant fraction of water in KG does not practically contain TFAA. This can be due to several reasons, such as poor accessibility of this intracellular water for TFAA or very low activity of interfacial clustered water (under strong confined space effects) as a solvent incapable to dissolve TFAA. Relative contribution of a fraction of water in the concentrated TFAA solution increases with decreasing temperature. Signal at 2 ppm can be attributed to WAW (Fig. 4 *c*) with $CDCl_3$ surroundings. Its relative intensity increases with decreasing temperature. In the case of stronger hydration sample (Fig. 4 *d*, solid lines), an increase in contribution of signal of concentrated solution of TFAA is observed.

The amounts of unfrozen water in KG *vs*. temperature depend on both water content and dispersion medium type (air or chloroform-d) (Fig. 5 *a*). This is well observed from the distribution functions of sizes of unfrozen water structures (Fig. 5 *b*) and related parameters

(Table 1) estimated for water unfrozen at $T < 273$ K.

The amounts of strongly (SBW) and weakly (WBW) bound waters can be determined from the $C_{uw}(T)$ functions assuming that WBW is frozen at 265 K < T < 273 K (since pure bulk water is frozen at 273.15 K). For soft matters, such as cells, microorganisms, relative contributions of SBW and WBW change not only due to changes in the total content of water but also due to changes in the organisation of macromolecules with increasing water content in the systems [9]. Therefore, at $h = 0.3$ g/g, the content of SBW is about only 16 % (Table 1), but at $h = 0.8$ g/g, it is equal to 29 %, and in chloroform-d, it increases to 40 %. These results can be explained by increasing "porosity" of KG with increasing content of water, especially at $R < 3$ nm (Fig. 5 *b*). The surface area in contact with unfrozen water increases with increasing value of h to 0.8 g/g (Table 1, S_{uw}). Contributions of both nanopores (S_{nano}) and mesopores (S_{meso}) increase. In the case of chloroform-d as dispersion medium, the structure of bound water strongly changes in comparison with air. This is due to a hydrophobic character of $CDCl_3$. Water and chloroform tend to reduce the contact area between immiscible liquids. Therefore, water form larger mesostructures (Fig. 5 *b*) and $S_{nano} = 0$ (Table 1). The value of $-\Delta G_s$ decreases but $<T_m>$ increases. Thus, water more weakly interacts with cellular structures because chloroform can displace water from narrow pores into larger ones. This is typical phenomenon for water/chloroform mixtures under confined space effects [9].

Table 1. Characteristics of water bound in kefir grains at $h = 0.3$ (in air) and 0.8 g/g (air and $CDCl_3$)

V_{nano} (cm^3/g)	V_{meso} (cm^3/g)	V_{macro} (cm^3/g)	V_{nano} (cm^3/g)	V_{meso} (cm^3/g)	V_{macro} (cm^3/g)	V_{nano} (cm^3/g)	V_{meso} (cm^3/g)	V_{macro} (cm^3/g)	V_{nano} (cm^3/g)
0	1.666	0.094	0	1.666	0.094	0	1.666	0.094	0
0.013	0.960	0.014	0.013	0.960	0.014	0.013	0.960	0.014	0.013
0.027	0.878	0.017	0.027	0.878	0.017	0.027	0.878	0.017	0.027

Note. ΔG_s is the Gibbs free energy of the most strongly bound water layer; $C_{uw}{}^{s}$ and $C_{uw}{}^{w}$ are the amounts of strongly and weakly bound waters, respectively; γ_S is the free surface energy determined as a modulus of whole changes in the Gibbs free energy of bound water; $<T_m>$ is the average melting temperature for bound water; S_{uw}, S_{nano} and S_{meso} are the specific surface area being in contact with unfrozen water, total, in nanopores and mesopores, respectively

Additional information on the temperature behaviour of water bound in KG differently hydrated can be obtained using DSC measurements [17]. DSC investigations of lactic acid bacteria showed occurrence of several processes including water freezing/melting and denaturation of biomacromolecules in organelles (ribosomes).

At a minimal content of water ($h = 0.3$ g/g), exotherms of freezing of water and some low-molecular weight organics (sugars, *etc*.) are observed between 263 and 273 K (Fig. 6 *a*) in contrast to a melting peak (Fig. 6 *b*). Only removal of baseline gives low-intensity endotherms used in thermoporometry (Fig. 7, curve 1). An increase in content of water, the shape of both freezing exotherms and melting endotherms becomes more complex. Note that the freezing exotherms shift toward lower temperatures at $h = 0.5$ and 0.7 g/g but at $h = 1$ g/g they shift toward higher temperatures. This effect is due to changes in contribution of weakly and strongly bound compounds observed in NMR measurements and the textural organisation of kefir grains at nano- and micro-scales. In other words, contribution of WBW increases at $h = 1$ g/g (Fig. 6 *a*). The endotherm effect value of water melting increases with increasing value of h (Table 2) but it is much lower than that for transformation of hexagonal ice/bulk water (330 J/g). This result can be caused by several reasons. First, there are many states of bound water frozen at different temperatures (*i.e.* melting of different ice crystallites or amorphous structures occurs over large temperature range). Second, the energy of interactions of water/water and water/biostructures in KG differs strongly in both directions. Therefore, total changes in phase transition of amorphous ice (bound water can form amorphous ice upon freezing) into bound water needs smaller energy than that for hexagonal ice transforming into bulk water.

Decane bound to dry KG has the freezing exotherm at 239 K (Fig. 6 *c*, curve 1) that is

lower than that for bulk *n*-decane (T_f = 242.5–243.8 K) due to confined space effects. In the case of a mixture of water and *n*-decane (added to hydrated KG at h = 0.2 g/g) bound to KG (Fig. 6 *c*, curve 2), the exotherm of decane freezing becomes broader and slightly shifts toward higher temperature. Consequently, water can locate in some narrow voids and decane cannot displace a portion of this water (crystallization peak at 273 K) from narrow voids. Therefore, the confined space effect for a fraction of bound decane becomes weaker in comparison with dry grains. Melting endotherms (Fig. 6 *d*) include besides a decane peak (around 244 K), some additional features (between 263 K and 253 K), which can be caused by low-molecular weight compounds (sugars, fat acids, phospholipids, residual water, *etc*.). In this temperature range, some small exotherms are also observed (Fig. 6 *c*).

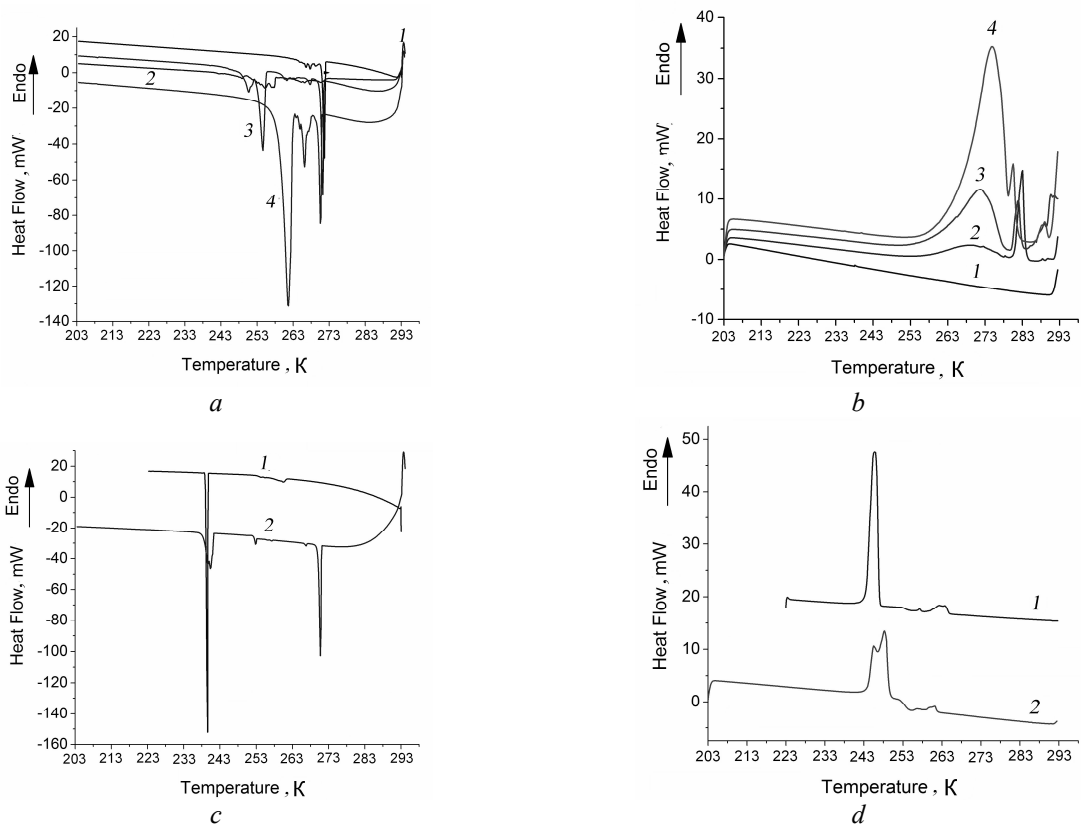

Fig. 6. (*a, b*) Freezing and (*c, d*) melting DSC thermograms for KG at different hydration degree h = (*a, b*) 0.3 (curve *1*), 0.5(*2*), 0.7(*3*) and 1 (*4*) g/g, and at (*c, d*) h = 0.2 g/g with addition of 0.2 g/g *n*-decane

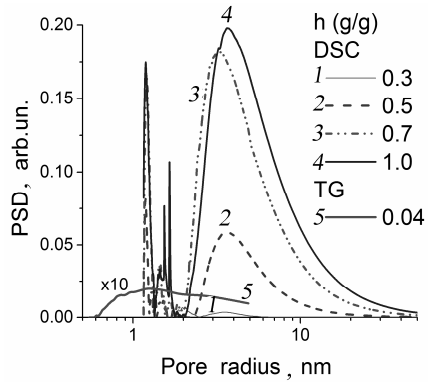

Fig. 7. Pore size distributions in KG calculated using DSC (curves *1-4* at h = 0.3, 0.5, 0.7, and 1 g/g, respectively) and TG (curve *5*, h = 0.04 g/g) thermoporometry

Table 2. Heat effect of melting of ice in frozen KG at various hydration degree

h, g/g	$\Delta H/T_{max}$, (J/g)/(K)		m_{H2O}, mg
0.3	3.7/268		14.26
0.5	5.4/269	6.7/277	32.64
0.7	28.3/269	3.1/277	29.87
1	38.6/271	1.61/276	50.46

CONCLUSIONS

Partially hydrated/dehydrated kefir grains include water structures in a broad range of sizes from small clusters (around 1 nm in size) to large nanodomains 10–50 nm in size. Changes in the hydration degree of kefir grains cause changes in their textural organisation. Contributions of weakly (δ_H = 1–2 ppm) and strongly (δ_H = 4–5.5 ppm) associated waters and weakly (frozen at 265 K < T < 273 K) and strongly (unfrozen at 200 K < T < 265 K) bound waters depend on the amounts of water and the type of dispersion medium (air, weakly polar chloroform, chloroform with addition of TFAA). The ratios between SAW/WAW and SBW/WBW depend on temperature since the larger the water structure (approaching to bulk water), the higher the freezing / melting temperature (approaching to 273 K). These water clusters and domains are characterised by different ability to dissolve such compounds as strong acids (F_3CCOOD studied as a representative). Enhanced clusterisation of water bound to kefir grains results in diminution of dissolution of the acid in this water.

ACKNOWLEDGEMENTS

The authors are grateful to European Community, Seventh Framework Programme (FP7/2007–2013), Marie Curie International Research Staff Exchange Scheme (IRSES grant No 612484) for financial support of this project.

Залежність стану води від температури в зернах кефіру при різній гідратації

В.М. Гунько, В.В. Туров, Т.В. Крупська, А.П. Головань, Є.М. Пахлов, М.Д. Цапко, J. Skubiszewska-Zięba, B. Charmas

Інститут хімії поверхні ім. О.О. Чуйка Національної академії наук України
вул. Генерала Наумова, 17, Київ, 03164, Україна, vlad_gunko@ukr.net
Київський національний університет імені Тараса Шевченка, хімічний факультет
вул. Володимирська, 64, Київ, 01030, Україна, nmrlab2007@ukr.net
Університет імені Марії Кюрі-Склодовської, хімічний факультет
пл. Марії Кюрі-Склодовської, 3, Люблін, 20031, Польща, jskubisz@o2.pl

Методами низькотемпературної ^{1}H ЯМР спектроскопії, ДСК і термогравіметрії досліджено вплив ступеня гідратації, дисперсного середовища (води, слабополярного розчинника $CDCl_3$, $CDCl_3$ + F_3CCOOD) і температури на властивості зв'язаної води в кефірних гранулах (КГ). Встановлено, що в результаті збільшення вмісту води, що додають до висушених КГ, змінюється структура води в супрамолекулярних структурах бактерій, низько- та високомолекулярних компонентів КГ. Виявлено п'ять типів води в КГ: (i) слабко асоційована вода, яка характеризується низьким значенням величини хімічного зсуву протонного резонансу δ_H = 1–2 м.ч.; (ii) сильно асоційована вода δ_H = 4–5.5 м.ч. (аналогічно об'ємній воді), (iii) слабко зв'язана вода, яка замерзає при 265 K < T < 273 K; (iv) сильно зв'язана вода, яка замерзає при 200 K < T < 265 K, та (v) об'ємна вода, яка безпосередньо не взаємодіє з бактеріями, клітинами, макромолекулами. ЯМР-кріопорометрія та термопорометрія, які базуються на методах ДСК і термогравіметрії, дають близькі результати та детально показують зміни в організації внутрішньоклітинної й позаклітинної води та інших низькомолекулярних сполук, при гідратації/дегідратації з додаванням слабкополярного ($CDCl_3$) чи сильнополярного компоненту (F_3CCOOD), при нагріванні чи замерзанні.

Ключові слова: *кефірні гранули, слабоасоційована та сильноасоційована вода*

Зависимость состояния воды от температуры в зернах кефира при различной гидратации

В.М. Гунько, В.В. Туров, Т.В. Крупская, А.П. Головань, Є.М. Пахлов, М.Д. Цапко, J. Skubiszewska-Zięba, B. Charmas

Институт химии поверхности им. А.А. Чуйко Национальной академии наук Украины ул. Генерала Наумова, 17, Киев, 03164, Украина, vlad_gunko@ukr.net
Киевский национальный университет имени Тараса Шевченко, химический факультет ул. Владимирская, 64, Киев, 01030, Украина, nmrlab2007@ukr.net
Университет имени Марии Кюри-Склодовской, химический факультет пл. Марии Кюри-Склодовской, 3, Люблин, 20031, Польша, jskubisz@o2.pl

Методами низкотемпературной ^{1}H ЯМР спектроскопии, ДСК и термогравиметрии изучено влияние степени гидратации, дисперсной среды (воды, слабополярного растворителя $CDCl_3$, $CDCl_3 + F_3CCOOD$) и температуры на свойства связанной воды в кефирных гранулах (КГ). Установлено, что в результате увеличения содержания воды, добавляемой к высушенным КГ, изменяется структура воды в супрамолекулярных структурах бактерий, низко- и высокомолекулярных компонентов КГ. Обнаружено пять типов воды в КГ: (i) слабо ассоциированная вода, которая характеризуется низким значением величины химического сдвига протонного резонанса δ_H = 1–2 м.д.; (ii) сильно ассоциированная вода δ_H = 4–5.5 м.д. (аналогично объемной воде), (iii) слабо связанная вода, которая замерзает при 265 K < T < 273 K; (iv) сильно связанная вода, которая замерзает при 200 K < T < 265 K; и (v) объемная вода, которая непосредственно не взаимодействует с бактериями, клетками, макромолекулами. ЯМР-криопорометрия и термопорометрия, базирующиеся на методах ДСК и термогравиметрии, дают близкие результаты, детально показывая изменения организации внутриклеточной и внеклеточной воды и других низкомолекулярных соединениях, при гидратации/дегидратации с добавлением слабополярного ($CDCl_3$) или сильно полярного компонента (F_3CCOOD), нагревании или замерзании.

Ключевые слова: *кефирные гранулы, слабоассоциированная и сильноассоциированная вода*

REFERENCES

1. Farnworth E.R. *Handbook of fermented functional foods*. (London: CRC Press, 2003).
2. Farnworth E.R. Kefir – a complex probiotic. *Food Science and Technology Bulletin: Functional foods.* 2005. **2**(1): 1.
3. Lopitz-Otsoa F., Rementeria A., Elguezabal N., Garaizar J. Kefir: a symbiotic yeasts-bacteria community with alleged healthy capabilities. *Rev. Iberoam. Micol.* 2006. **23**(2): 67.
4. Silva K.R., Rodrigues S.A., Xavier L., Lima A.S. Antimicrobial activity of broth fermented with kefir grains. *Appl. Biochem. Biotechnol.* 2009. **152**(2): 316.
5. Adriana P., Socaciu C. Probiotic activity of mixed cultures of kefir's lactobacilli and non-lactose fermenting yeasts. *Bulletin UASVM, Agriculture*. 2008. **65**(2): 1843.
6. Chen Z., Shi J., Yang X., Nan B., Liu Y., Wang Z. Chemical and physical characteristics and antioxidant activities of the exopolysaccharide produced by Tibetan kefir grains during milk fermentation. *Int. Dairy J.* 2015. **43**: 15.
7. (a) Goff H.D. Colloidal aspects of ice-cream: a review. *Int. Dairy J.* 1997. **7**(6–7): 363;
   (b) Schuck P., Davenel A., Mariette F., Briard V., Méjean S., Piot M. Rehydration of casein powders: Effects of added mineral salts and salt addition methods on water transfer. *Int. Dairy J.* 2002. **12**(1): 51;
   (c) Lucas T., Le Ray D., Barey P., Mariette F. NMR assessment of ice cream: Effect of formulation on liquid and solid fat. *Int. Dairy J.* 2005. **15**(12): 1225;
   (d) Fuquay J.W., Fox P.F., McSweeney P.L.H. (Eds.) *Encyclopedia of Dairy Sciences*. 2nd Edition. (Oxford: Academic Press, 2011).
8. (a) Franks F. *Biophysics and biochemistry at low temperature*. (Cambridge: University Press, 1985);
   (b) Coulibaly I., Dubois-Dauphin R., Destain J., Fauconnier M.-L., Lognay G., Thonart P. The resistance to freeze-drying and to storage was determined as the cellular ability to recover its survival rate and acidification activity. *International Journal of Microbiology*. 2010. **2010**: 625239.
9. Gun'ko V.M., Turov V.V. *Nuclear magnetic resonance studies of interfacial phenomena*. (Boca Raton: CRC Press, 2013).
10. (a) Chaplin M. *Water structure and science.* 2015. http://www.lsbu.ac.uk/water/;

(b) Gaspar P., Carvalho A.L., Vinga S., Santos H., Neves A.R. From physiology to systems metabolic engineering for the production of biochemicals by lactic acid bacteria. *Biotechnol. Adv.* 2013. **31**(6): 764;
(c) Crowley S., Mahony J., van Sinderen D. Current perspectives on antifungal lactic acid bacteria as natural bio-preservatives. *Trends in Food Science & Technology*. 2013. **33**(2): 93;
(d) Tsakalidou E., Papadimitriou K. *Stress responses of lactic acid bacteria*. (Springer Science & Business Media, 2011);
(e) Hofvendahl K., Hahn–Hägerdal B. Factors affecting the fermentative lactic acid production from renewable resources. *Enzyme Microb. Technol.* 2000. **26**(2–4): 87;
(f) Toy N., Özogul F., Özogul Y. The influence of the cell free solution of lactic acid bacteria on tyramine production by food borne-pathogens in tyrosine decarboxylase broth. *Food Chem.* 2015. **173**: 45;
(g) Jennings T.A. *Lyophilization: Introduction and Basic Principles*. (Boca Raton: Interpharm/CRC, 2002);
(h) Chen Z., Kang L., Wang Z., Xu F., Gu G., Cui F., Guo Z. Recent progress in the research of biomaterials regulating cell behavior. *RSC Adv.* 2014. **4**: 63807;
(i) Mellati A., Dai S., Bi J., Jin B., Zhang H. A biodegradable thermosensitive hydrogel with tuneable properties for mimicking threedimensional microenvironments of stem cells. *RSC Adv*. 2014. **4**: 63951.

11. Mitchell J., Webber J.B.W., Strange J.H. Nuclear magnetic resonance cryoporometry. *Phys. Rep.* 2008. **461**(1): 1.
(a) Wunderlich B. *Thermal analysis*. (New York: Academic Press, 1990);
(b) Bertram H.C., Wiking L., Nielsen J.H., Andersen H.J. Direct measurement of phase transitions in milk fat during cooling of cream – a low-field NMR approach. *Int. Dairy J.* 2005. **15**(10): 1056;
(c) Métais A., Cambert M., Riaublanc A., Mariette F. Influence of fat globule membrane composition on water holding capacity and water mobility in casein rennet gel: A nuclear magnetic resonance self-diffusion and relaxation study. *Int. Dairy J.* 2006. **16**(4): 344;
(d) Berner D., Viernstein H. Effect of protective agents on the viability of Lactococcus lactis subjected to freeze-thawing and freeze-drying. *Sci. Pharm.* 2006. **74**: 137;
(e) Salomonsen T., Sejersen M.T., Viereck N., Ipsen R., Engelsen S.B. Water mobility in acidified milk drinks studied by low-field ^{1}H NMR. *Int. Dairy J.* 2007. **17**(4): 294;
(f) Van lent K., Vanlerberghe B., Van Oostveldt P., Thas O., Van der Meeren P. Determination of water droplet size distribution in butter: Pulsed field gradient NMR in comparison with confocal scanning laser microscopy. *Int. Dairy J.* 2008. **18**(1): 12;
(g) Noronha N., Duggan E., Ziegler G.R., O'Riordan E.D., O'Sullivan M. Investigation of imitation cheese matrix development using light microscopy and NMR relaxometry. *Int. Dairy J.* 2008. **18**(6): 641;
(h) Grivet J.-P., Delort A.-M. NMR for microbiology: *In vivo* and *in situ* applications. *Prog. Nucl. Magn. Reson. Spectrosc.* 2009. **54**(1): 1;
(i) Kaufmann N., Andersen U., Wiking L. Shear and rapeseed oil addition affect the crystal polymorphic behavior of milk fat. *J. Am. Oil Chem. Soc.* 2013. **90**(6): 871;
(j) Mikhalovska L.I., Gun'ko V.M., Rugal A.A., Oranska O.I., Gornikov Yu.I., Morvan C., Domas C., Mikhalovsky S.V. Cottonised flax fibres vs. cotton fibres: structural, textural and adsorption characteristics. *RSC Adv.* 2012. **2**: 2032;
(k) Bershtein V.A., Gun'ko V.M., Egorova L.M., Wang Z., Illsley M., Voronin E.F., Prikhod'ko G.P., Yakushev P.N., Leboda R., Skubiszewska-Zięba J. and Mikhalovsky S.V. Dynamics, thermal behaviour and elastic properties of thin films of poly(vinyl alcohol) nanocomposites. *RSC Adv.* 2012. **2**: 1424;
(l) Bershtein V.A., Gun'ko V.M., Karabanova L.V., Sukhanova T.E., Yakushev P.N., Egorova L.M., Turova A.A., Zarko V.I., Pakhlov E.M., Vylegzhanina M.E., Mikhalovsky S.V. Polyurethane–poly(2-hydroxyethyl methacrylate) semi-IPN–nanooxide composites. *RSC Adv.* 2013. **3**: 14560;
(m) Mikhalovsky S.V., Gun'ko V.M., Bershtein V.A., Turov V.V., Egorova L.M., Morvan C., Mikhalovska L.I. A comparative study of air-dry and water swollen flax and cotton fibres. *RSC Adv.* 2012. **2**: 2868.

12. (a) Gun'ko V.M., Turov V.V., Bogatyrev V.M., Zarko V.I., Leboda R., Goncharuk E.V., Novza A.A., Turov A.V., Chuiko A.A. Unusual properties of water at hydrophilic/hydrophobic interfaces. Advances in Colloid and Interface Science. 2005. **118**(1–3): 125;
(b) Gun'ko V.M., Turov V.V., Krupska T.V., Tsapko M.D., Skubiszewska-Zięba J., Charmas B., Leboda R. Effects of strongly aggregated silica nanoparticles on interfacial behaviour of water bound to lactic acid bacteria. *RSC Adv.* 2015. **5**: 7734.

13. (a) Hay J.N., Laity P.R. Observations of water migration during thermoporometry studies of cellulose films. *Polymer*. 2000. **41**(16): 6171;
(b) Landry M.R. Thermoporometry by differential scanning calorimetry: experimental considerations and applications. *Thermochim. Acta*. 2005. **433**(1–2): 27.

14. (a) Goworek J., Stefaniak W., Zgrajka W. Measuring porosity of polymeric adsorbents by temperature programmed desorption of liquids. *Mater. Chem.Phys.* 1999. **59**(2): 149;

(b) Goworek J., Stefaniak W., Prudaczuk M. The influence of polarity of liquids on the parameters characterising the porosity of silica gels estimated by thermogravimetric analysis. *Thermochim. Acta.* 2001. **379**(1–2): 117;
(c) Gun'ko V.M., Goncharuk O.V., Goworek J. Evaporation of polar and nonpolar liquids from silica gels and fumed silica. Colloids Surf., A. 2015. **474**: 52.

15. Abragam A. *The principles of nuclear magnetism*. (Oxford: Oxford University Press, 1961).
16. (a) Höhne G., Hemminger W., Flammersheim H.-J. *Differential scanning calorimetry – An introduction for practitioners*. (Springer-Verlag, 1996);
(b) Lee J., Kaletunç G. Evaluation of the heat inactivation of Escherichia coli and Lactobacillus plantarum by differential scanning calorimetry. *Appl. Environ. Microbiol*. 2002. **68**(11): 5379;
(c) Mohacsi-Farkas C., Farkas J., Meszaros L., Reichart O., Andrassy E. Thermal denaturation of bacterial cells examined by differential scanning calorimetry. *J. Therm. Anal. Calorim*. 1999. **57**(2): 409.

Received 05.06.2015, accepted 24.11.2015